J|A|C|S ARTICLES

Published on Web 11/19/2010

Tyrosine−Lipid Peroxide Adducts from Radical Termination: Para Coupling and Intramolecular Diels−Alder Cyclization

Roman Shchepin,[†] Matias N. Möller,[†,‡] Hye-young H. Kim,[†] Duane M. Hatch,[†] Silvina Bartesaghi,[§] Balaraman Kalyanaraman,[∥] Rafael Radi,[⊥] and Ned A. Porter*[,†]

Department of Chemistry and Vanderbilt Institute of Chemical Biology, Vanderbilt University, Nashville, Tennessee 37235, United States, Facultad de Ciencias and Center for Free Radical and Biomedical Research, Universidad de la República, Montevideo, Uruguay, Departamento de Histología and Center for Free Radical and Biomedical Research, Facultad de Medicina, Universidad de la República, Montevideo, Uruguay, Department of Biophysics and Free Radical Research Center, Medical College of Wisconsin, Milwaukee, Wisconsin 53226, United States, and Departamento de Bioquímica, Facultad de Medicina, Universidad de la República, Montevideo, Uruguay

Received July 22, 2010; E-mail: n.porter@vanderbilt.edu

Abstract: Free radical co-oxidation of polyunsaturated lipids with tyrosine or phenolic analogues of tyrosine gave rise to lipid peroxide−tyrosine (phenol) adducts in both aqueous micellar and organic solutions. The novel adducts were isolated and characterized by 1D and 2D NMR spectroscopy as well as by mass spectrometry (MS). The spectral data suggest that the polyunsaturated lipid peroxyl radicals give stable peroxide coupling products exclusively at the para position of the tyrosyl (phenoxy) radicals. These adducts have characteristic ^{13}C chemical shifts at 185 ppm due to the cross-conjugated carbonyl of the phenol-derived cyclohexadienone. The primary peroxide adducts subsequently undergo intramolecular Diels−Alder (IMDA) cyclization, affording a number of diastereomeric tricyclic adducts that have characteristic carbonyl ^{13}C chemical shifts at ∼198 ppm. All of the NMR HMBC and HSQC correlations support the structure assignments of the primary and Diels−Alder adducts, as does MS collision-induced dissociation data. Kinetic rate constants and activation parameters for the IMDA reaction were determined, and the primary adducts were reduced with cuprous ion to give a phenol-derived 4-hydroxycyclohexa-2,5-dienone. No products from adduction of peroxyls at the phenolic ortho position were found in either the primary or cuprous reduction product mixtures. These studies provide a framework for understanding the nature of lipid−protein adducts formed by peroxyl−tyrosyl radical−radical termination processes. Coupling of lipid peroxyl radicals with tyrosyl radicals leads to cyclohexenone and cyclohexadienone adducts, which are of interest in and of themselves since, as electrophiles, they are likely targets for protein nucleophiles. One consequence of lipid peroxyl reactions with tyrosyls may therefore be protein−protein cross-links via interprotein Michael adducts.

Introduction

Protein-derived tyrosine radicals can act as cofactors in some enzymatic reactions, including those of class I ribonucleotide reductase, prostaglandin H synthase, photosystem II,[1,2] and cytochrome C oxidase.[3] On the other hand, protein-derived tyrosyl radicals can also be formed in vivo as a result of oxidative stress through mechanisms including both free radical[4−7] and hemeperoxidase-dependent[8] oxidations. Tyrosine nitration, for example, is thought to occur by a two-step reaction involving the initial formation of a tyrosyl radical that subsequently reacts with nitrogen dioxide (Scheme 1).[4,9−11] The formation of 3-nitrotyrosine is an important protein post-translational modification that can alter structure and function.[12] It is associated with acute and chronic disease states and can be a predictor of disease risk and progression.[11,13] The extent of protein tyrosine

[†] Vanderbilt University.
[‡] Facultad de Ciencias and Center for Free Radical and Biomedical Research, Universidad de la República.
[§] Departamento de Histología, and Center for Free Radical and Biomedical Research, Facultad de Medicina, Universidad de la República.
[∥] Medical College of Wisconsin.
[⊥] Departamento de Bioquímica, Facultad de Medicina, Universidad de la República.

(1) Pesavento, R. P.; van der Donk, W. A. *Adv. Protein Chem.* **2001**, *58*, 317.
(2) Hoganson, C. W.; Tommos, C. *Biochim. Biophys. Acta* **2004**, *1655*, 116.
(3) Proshlyakov, D. A.; Pressler, M. A.; DeMaso, C.; Leykam, J. F.; DeWitt, D. L.; Babcock, G. T. *Science* **2000**, *290*, 1588.
(4) Radi, R. *Proc. Natl. Acad. Sci. U.S.A.* **2004**, *101*, 4003.
(5) Das, A. B.; Nagy, P.; Abbott, H. F.; Winterbourn, C. C.; Kettle, A. J. *Free Radical Biol. Med.* **2010**, *48*, 1540.
(6) Nagy, P.; Kettle, A. J.; Winterbourn, C. C. *J. Biol. Chem.* **2009**, *284*, 14723.
(7) Winterbourn, C. C. *Nat. Chem. Biol.* **2008**, *4*, 278.
(8) Heinecke, J. W. *Toxicology* **2002**, *177*, 11.
(9) Bartesaghi, S.; Wenzel, J.; Trujillo, M.; Lopez, M.; Joseph, J.; Kalyanaraman, B.; Radi, R. *Chem. Res. Toxicol.* **2010**, *23*, 821.
(10) Bartesaghi, S.; Valez, V.; Trujillo, M.; Peluffo, G.; Romero, N.; Zhang, H.; Kalyanaraman, B.; Radi, R. *Biochemistry* **2006**, *45*, 6813.
(11) Szabo, C.; Ischiropoulos, H.; Radi, R. *Nat. Rev. Drug. Discovery* **2007**, *6*, 662.
(12) Ischiropoulos, H. *Arch. Biochem. Biophys.* **2009**, *484*, 117.
(13) Peluffo, G.; Radi, R. *Cardiovasc. Res.* **2007**, *75*, 291.

 10.1021/ja106503a

Scheme 1. Free-Radical-Mediated Tyrosine Oxidation Reactions

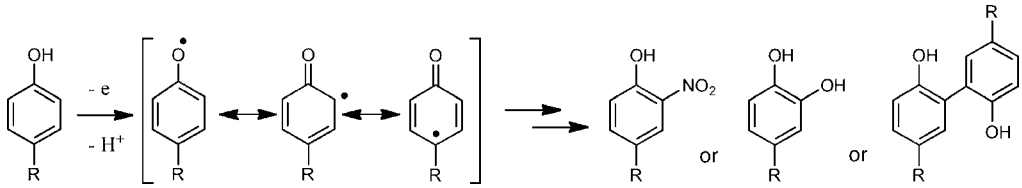

nitration depends on the particular protein structure and the environment and location of the individual tyrosine residue.[14]

Tyrosyl radicals also couple to form 3,3′-dityrosine[15−17] (see Scheme 1), and the formation of tyrosine dimers is frequently cited as evidence for the formation of tyrosyl radical species in vivo. Dimerization has been associated with protein cross-linking and the formation of high-molecular-weight species.[16,17]A recent report, for example, showed that dimerization of a SLC30A family of zinc transporters depends on redox-regulated covalent tyrosine dimerization and suggested that dityrosine-dependent membrane protein oligomerization may regulate the function of diverse membrane proteins in normal and disease states.[18]

Most of the mechanistic studies of tyrosine nitration and dimerization have been carried out under aqueous conditions, but the same chemistry has been observed in tyrosine-containing proteins that interact with membrane lipids or are located in hydrophobic environments.[14,19] It is important to note that tyrosines are frequently observed in membrane-binding regions of proteins, and a recent analysis has suggested that placement of tyrosine residues in protein membrane locations minimizes the free energy relative to their placement in solvent-exposed or transitional sites.[20] The colocalization of tyrosine protein residues and membrane lipids suggests the possibility of reactions of tyrosyl and lipid-derived radicals,[9,10] since membranes, particularly those containing polyunsaturated fatty acid (PUFA)[21] esters,[22−24] are subject to peroxidation via chain-carrying peroxyl free radicals. Membrane lipid peroxidation has been linked to a number of human diseases, including atherosclerosis[25,26] and neurodegenerative disorders.[27−30] It is notable that simultaneous lipid peroxidation, tyrosine dimerization, and protein tyrosine nitration have been observed in red blood cell membranes, indicating that these competing processes occur even in membranes that contain α-tocopherol.[31]

Scheme 2. Primary Coupling Products of Tyrosyl and Lipid Peroxyl Radicals

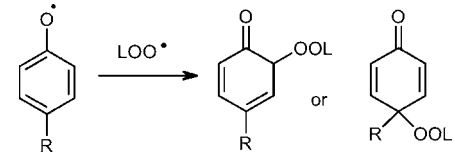

Oxidation of tyrosine residues in ApoA1, a principal constituent of high-density lipoprotein (HDL), has been of particular interest because HDL plays an important role in the transport of cholesterol from peripheral tissues to the liver. Recent studies have provided evidence that oxidative modification of ApoA1 leads to loss of HDL function.[32,33] Modification of HDL tyrosines by nitration or chlorination has been the principal focus of most studies, but HDL tyrosines are also prime targets for peroxidative modification since HDLs are lipid- and protein-rich but poorly protected from peroxyl free radicals by nature's antioxidant, α-tocopherol.[34,35]

Here we report studies of lipid peroxyl coupling with alkylphenoxy radicals that serve as models for tyrosyls (see Scheme 2). The product mixture formed in a reaction of this type is complex and includes dialkyl peroxide coupling compounds as well as novel Diels−Alder adducts. It seems likely that products similar to the ones identified here are major products in the free radical peroxidation of tyrosine-containing membranes, since cross-termination has been established as a major pathway in radical reactions involving both peroxyl and phenoxy species.[36]

Results

Co-oxidation of Hydrophobic Tyrosine (1) with 1-Palmitoyl-(13*S*)-hydroperoxyoctadecadienoylglycerylphosphatidylcholine (2). The hydrophobic tyrosine analogue[10,37] *N-t*-BOC-L-tyrosine *tert*-butyl ester (BTBE, **1**; 2 mM) was mixed with enantiopure

(14) Bartesaghi, S.; Ferrer-Sueta, G.; Peluffo, G.; Valez, V.; Zhang, H.; Kalyanaraman, B.; Radi, R. *Amino Acids* **2007**, *32*, 501.
(15) Dean, R. T.; Fu, S.; Stocker, R.; Davies, M. J. *Biochem. J.* **1997**, *324*, 1.
(16) Souza, J. M.; Peluffo, G.; Radi, R. *Free Radical Biol. Med.* **2008**, *45*, 357.
(17) Giulivi, C.; Traaseth, N. J.; Davies, K. J. *Amino Acids* **2003**, *25*, 227.
(18) Salazar, G.; Falcon-Perez, J. M.; Harrison, R.; Faundez, V. *PLoS One* **2009**, *4*, e5896.
(19) Shao, B.; Bergt, C.; Fu, X.; Green, P.; Voss, J. C.; Oda, M. N.; Oram, J. F.; Heinecke, J. W. *J. Biol. Chem.* **2005**, *280*, 5983.
(20) Koehler, J.; Woetzel, N.; Staritzbichler, R.; Sanders, C. R.; Meiler, J. *Proteins* **2009**, *76*, 13.
(21) Abbreviations: PUFA, polyunsaturated fatty acid; NMR, nuclear magnetic resonance; MeOAMVN, 2,2′-azobis(4-methoxy-2,4-dimethylvaleronitrile); HPLC, high-performance liquid chromatography; EtOAc, ethyl acetate; DMF, *N*,*N*-dimethylformamide; MS, mass spectrometry; HSQC, heteronuclear single-quantum coherence; HMBC, heteronuclear multiple-bond coherence; NOE, nuclear Overhauser effect; NOESY, NOE spectroscopy; ESI, electrospray ionization; TIC, total ion current; *m*/*z*, mass-to-charge ratio; IMDA, intramolecular Diels−Alder; BTBE, *N-t*-BOC-L-tyrosine *tert*-butyl ester; PLPC, 1-palmitoyl-2-linoleoylglycerylphosphatidylcholine.
(22) Porter, N. A. *Acc. Chem. Res.* **1986**, *19*, 262.
(23) Porter, N. A. *Methods Enzymol.* **1984**, *105*, 273.
(24) Xu, L.; Davis, T. A.; Porter, N. A. *J. Am. Chem. Soc.* **2009**, *131*, 13037.
(25) Leeuwenburgh, C.; Rasmussen, J. E.; Hsu, F. F.; Mueller, D. M.; Pennathur, S.; Heinecke, J. W. *J. Biol. Chem.* **1997**, *272*, 3520.
(26) Yoritaka, A.; Hattori, N.; Uchida, K.; Tanaka, M.; Stadtman, E. R.; Mizuno, Y. *Proc. Natl. Acad. Sci. U.S.A.* **1996**, *93*, 2696.
(27) Ames, B. N. *Mutat. Res.* **2001**, *475*, 7.
(28) Beckman, K. B.; Ames, B. N. *Physiol. Rev.* **1998**, *78*, 547.
(29) Giasson, B. I.; Duda, J. E.; Murray, I. V. J.; Chen, Q.; Souza, J. M.; Hurtig, H. I.; Ischiropoulos, H.; Trojanowski, J. Q.; Lee, V. M. *Science* **2000**, *290*, 985.
(30) Montine, T. J.; Huang, D. Y.; Valentine, W. M.; Amarnath, V.; Saunders, A.; Weisgraber, K. H.; Graham, D. G.; Strittmatter, W. J. *J. Neuropathol. Exp. Neurol.* **1996**, *55*, 202.
(31) Romero, N.; Peluffo, G.; Bartesaghi, S.; Zhang, H.; Joseph, J.; Kalyanaraman, B.; Radi, R. *Chem. Res. Toxicol.* **2007**, *20*, 1638.
(32) Wu, Z.; Wagner, M. A.; Zheng, L.; Shy, J. M.; Smith, J. D.; Gogonea, V.; Hazen, S. L. *Nat. Struct. Mol. Biol.* **2007**, *14*, 861.
(33) Shao, B.; Oda, M. N.; Oram, J. F.; Heinecke, J. W. *Chem. Res. Toxicol.* **2010**, *23*, 447.
(34) Schaefer, E. J.; Foster, D. M.; Jenkins, L. L.; Lindgren, F. T.; Berman, M.; Levy, R. I.; Brewer, H. B. *Lipids* **1979**, *14*, 511.
(35) Karlsson, H.; Leanderson, P.; Tagesson, C.; Lindahl, M. *Proteomics* **2005**, *5*, 1431.
(36) Bravo, A.; Bjørsvik, H.; Fontana, F.; Liguori, L.; Minisci, F. *J. Org. Chem.* **1997**, *62*, 3849.

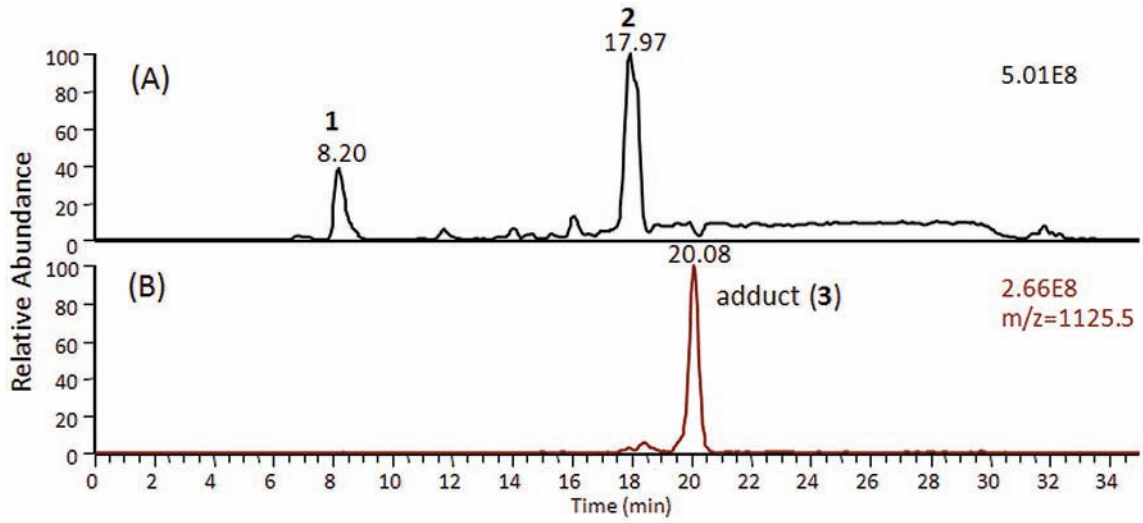

Figure 1. HPLC−MS analysis of the reaction mixture for the reaction of BTBE (**1**) and PLPC-(13*S*)-OOH (**2**). (A) Total ion current of the reaction mixture. The early-eluting peak at 8.2 min is **1**, and the later-eluting peak at 18.0 min is **2**. Reversed-phase HPLC on C-18 with solvents A (10 mM NH_4OAc in H_2O) and B (10 mM NH_4OAc in 95% CH_3OH/H_2O) was used, with the gradient starting at 70% B, going to 100% B over 10 min, and remaining at 100% B for 15 min. (B) Extracted ion current detecting the adduct **3** (*m*/*z* 1125.5).

PLPC-(13*S*)-hydroperoxide (**2**; 6.8 mM) generated by reaction of the 2-linoleoylglycerophospholipid with soybean lipoxygenase. The mixture was sonicated at room temperature to form micelles in the presence of the azo free radical initiator 2,2′-azobis(4-methoxy-2,4-dimethylvaleronitrile) (MeOAMVN; 1 mM). The micellar solution was allowed to stand in a 37 °C sand bath for 4 h and then analyzed by HPLC−MS. A typical chromatogram is presented in Figure 1.

MS analysis indicated the formation of adduct(s) having a parent ion at *m*/*z* 1125.5, corresponding to the expected mass of adduct **3**. However, attempts to isolate and further characterize the adduct(s) proved futile because the initial products were only moderately stable and appeared to undergo further transformations upon attempted purification. Furthermore, the yield of the *m*/*z* 1125 adduct(s) formed under the micellar conditions was low, and the products were not well-behaved on silica gel. For these reasons, we sought to simplify both the tyrosine (phenol) and membrane lipid reactants to allow any lipid-tyrosine adducts formed to be isolated on a scale that would permit characterization of the products by the normal tools of organic chemistry, including two-dimensional (2D) NMR spectroscopy.

Examination of the reactions of several tyrosine derivatives with the simplest oxidizable fatty acids (or esters) still gave complex mixtures of products that were difficult to purify. The final simplification of the tyrosine model was to reduce the complexity by using the phenol (7-methoxy-2-oxo-2*H*-chromen-4-yl)methyl 3-(4-hydroxyphenyl)propanoate (**4**), a compound that has no stereogenic center but does possess a built-in chromophore unrelated to the oxidizable tyrosine moiety. The compound, which was prepared in one step in 87% yield, provided a model substrate having $\lambda_{max} = 330$ nm that could be used as a tag for products derived from the phenol. The fatty acid component was also simplified in order to minimize the number of isomeric products generated during the oxidation reaction. This reduction of complexity of the system studied led to a series of reactions of the azo-initiated co-oxidation of phenol **4** with the symmetrical diene (6*E*,9*E*)-pentadecadiene (**5**).[38]

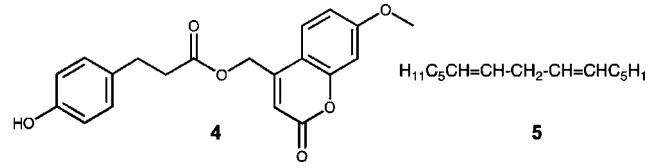

Peroxide Adducts of Peroxyl−Phenoxy Coupling. UV-active tyrosine analogue **4** was co-oxidized with diene **5** in benzene for 9 h at 37 °C using MeOAMVN as the initiator. The reaction progress was monitored at 330 nm by normal-phase (NP) HPLC−UV using 25% ethyl acetate in hexanes as the mobile phase (Figure 2A). In the early stages of oxidation, a peak at 16 min appeared (fraction IV), while additional peaks were detected at longer reaction times. The peak at 16 min (Figure 2A, fraction IV) was collected, evaporated to dryness, and resuspended in 1:1 H_2O/acetonitrile. Reversed-phase (RP) HPLC of fraction IV (Figure 2B) showed it to be homogeneous; the purified compound was dissolved in $CDCl_3$, and ^1H, COSY, NOESY, HSQC, HMBC, and ^{13}C spectra were obtained at room temperature. The spectral data acquired for fraction IV led to the assignment of structure **6** for this major product of the co-oxidation reaction. Compound **6** has a characteristic ^{13}C chemical shift for the carbonyl carbon (C4) at 185 ppm, and in the HMBC experiment, C4 exhibited only one three-bond cross-peak to H2. Extraction of coupling constants suggested that the conjugated diene has *E*,*E* geometry, and the integration and coupling pattern were consistent with the proposed peroxyl−phenoxy para-coupling product.

The adduct **6** was found to be unstable, and it formed a mixture of stereoisomeric products with structures assigned as the intramolecular Diels−Alder (IMDA) cyclization products **7a**−**c**. The same NP−RP protocol used to purify **6** was also used to isolate the stereoisomeric IMDA products. Thus, the

(37) Zhang, H.; Joseph, J.; Feix, J.; Hogg, N.; Kalyanaraman, B. *Biochemistry* **2001**, *40*, 7675.

(38) Tallman, K. A.; Roschek, B.; Porter, N. A. *J. Am. Chem. Soc.* **2004**, *126*, 9240.

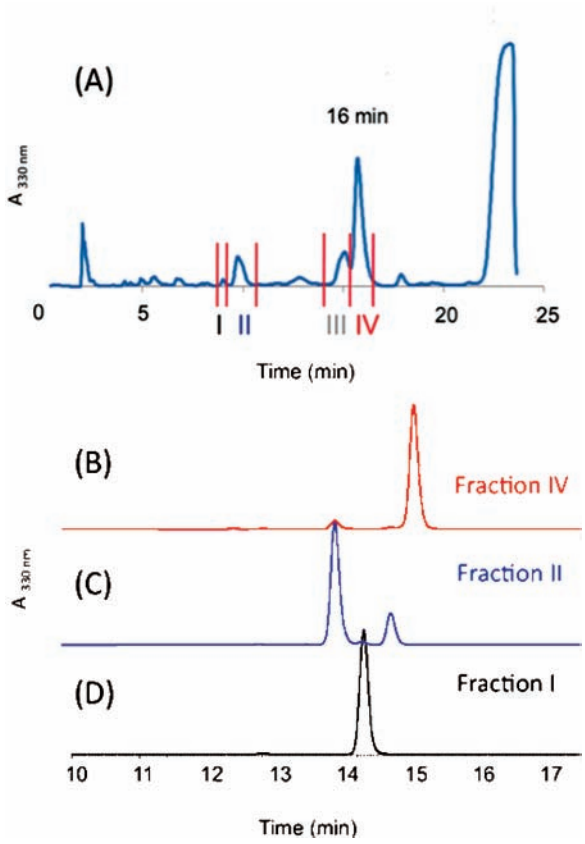

Figure 2. HPLC−UV (330 nm) analysis of the co-oxidation reaction of **4** and **5**. (A) Normal-phase separation of the reaction mixture into fractions I−IV (**4** elutes at 23 min). (B−D) Reversed-phase analyses of the separated fractions IV, II, and I.

reaction mixture was first purified with NP HPLC to collect the acyclic and cyclic adduct fractions, and the peaks collected as fractions I−IV were then analyzed for purity with RP HPLC. Fraction I contained only one product, **7a**, which eluted at 14.3 min in the RP HPLC step (Figure 2D), and fraction II separated into two peaks that eluted at 14.1 (**7b**) and 14.9 (**7c**) min. (Figure 2C). It is noteworthy that all of the IMDA products **7a**−**c** were formed from the single peroxide precursor **6** (i.e., fraction IV).

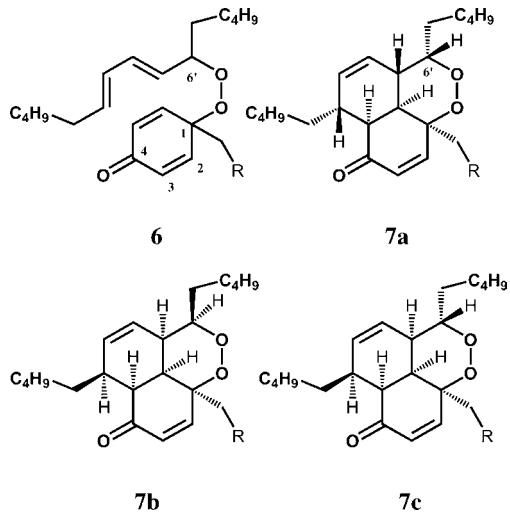

Fraction III could not be separated completely from fraction IV and appeared to be a product closely related to **6**. Thus, NMR analysis of fraction III (Figure S5 in the Supporting Information) showed it to be a mixture of compounds that are isomeric with **6** at the conjugated diene center adjacent to C6′. The suggested structures have one of the double bonds of the conjugated structure in the *Z* configuration. The MS and UV analyses of fraction III are consistent with the structures of the proposed constituents.

Distinctive differences between the para-coupling and IMDA adducts can be seen not only in the ^{13}C chemical shifts but also in the HMBC correlations. As noted above, the ^{13}C chemical shift for the carbonyl carbon (C4) of **6** was observed at 185 ppm, while those of the IMDA products were generally seen at 199 ppm. In the HMBC experiment, C4 of **6** exhibited only one three-bond cross-peak to H2, whereas each cyclic adduct gave rise to two additional cross-peaks to the ring-junction protons, as shown in Figure 3. The stereochemistry of each IMDA adduct was assigned on the basis of NOESY correlations between protons that are within the allowed spatial vicinity.

HSQC spectra provide one-bond correlations between carbons and protons along with the number of attached protons. The ^{13}C signals of the peroxide-bearing carbons of **6** and the IMDA adducts showed only one HSQC cross-peak, corresponding to C6′ at 86.0 ppm for **6** and 82.2 ppm for the diastereomeric adducts **7**. Any ortho-coupling adducts such as **8** or potential derivative IMDA products such as **9** and **10**[39−43] would exhibit two HSQC cross-peaks for both C5 and C6′ in each adduct. We therefore conclude that significant amounts of stable ortho-coupling products were not formed. Both the HSQC and HMBC spectra therefore support the notion that para coupling of the phenoxy and peroxyl radicals occurs, forming adducts **6** and **7a**−**c** as the major stable adducts. A more detailed discussion of the NMR analyses is presented in the Supporting Information.

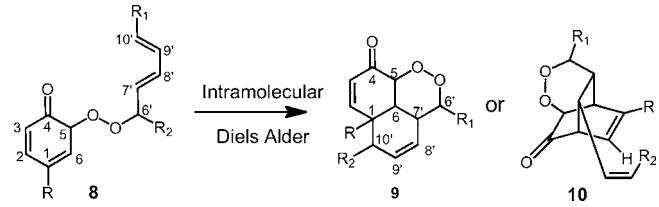

Silver-Coordinated (LC−Ag^+)-CID-MS Analysis of Acyclic and Cyclic Adducts. While molecular-ion MS information for the adducts was collected using electrospray ionization (ESI) and atmospheric pressure chemical ionization (APCI) methods, good collision-induced dissociation (CID) spectra could not be obtained by these conventional approaches. Silver ion forms stable complexes with unsaturated compounds, and silver-ion-coordination MS proved to be a useful approach to provide additional support for the assigned structures of **6** and **7**. For all of the isolated adducts, precursor masses of at *m*/*z* 699 and 701 [M + Ag] due to the two isotopes ^{107}Ag and ^{109}Ag were observed (Figure 4A). The silver ion complex of the primary adduct **6** displayed a major fragment ion at *m*/*z* 476 [M − 223 + Ag] due to cleavage of the peroxide bond (Figure

(39) Masuda, T.; Bando, H.; Maekawa, T.; Takeda, Y.; Yamaguchi, H. *Tetrahedron Lett.* **2000**, *41*, 2157.
(40) Masuda, T.; Maekawa, T.; Hidaka, K.; Bando, H.; Takeda, Y.; Yamaguchi, H. *J. Agric. Food Chem.* **2001**, *49*, 2539.
(41) Masuda, T.; Yamada, K.; Akiyama, J.; Someya, T.; Odaka, Y.; Takeda, Y.; Tori, M.; Nakashima, K.; Maekawa, T.; Sone, Y. *J. Agric. Food Chem.* **2008**, *56*, 5947.
(42) Masuda, T.; Yamada, K.; Maekawa, T.; Takeda, Y.; Yamaguchi, H. *Food Sci. Technol. Res.* **2006**, *12*, 173.
(43) Masuda, T.; Yamada, K.; Maekawa, T.; Takeda, Y.; Yamaguchi, H. *J. Agric. Food Chem.* **2006**, *54*, 6069.

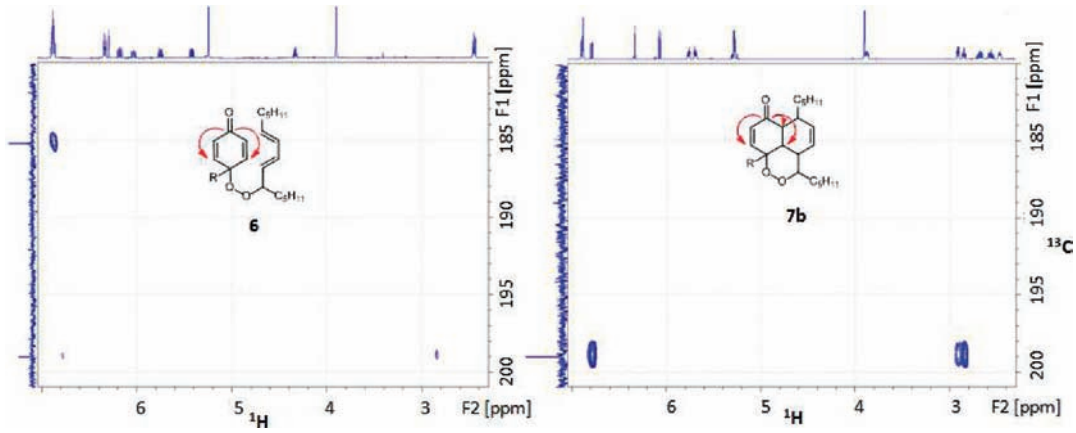

Figure 3. Representative HMBC correlations in adducts **6** and **7b**. (left) Adduct **6**: C4 (185 ppm) to H2 (6.8 ppm). (right) Adduct **7b**: C4 (199 ppm) to H2 (6.8 ppm) and H6 (2.9 and 2.8 ppm). There is also a weak two-bond correlation to H5 with this diastereomer.

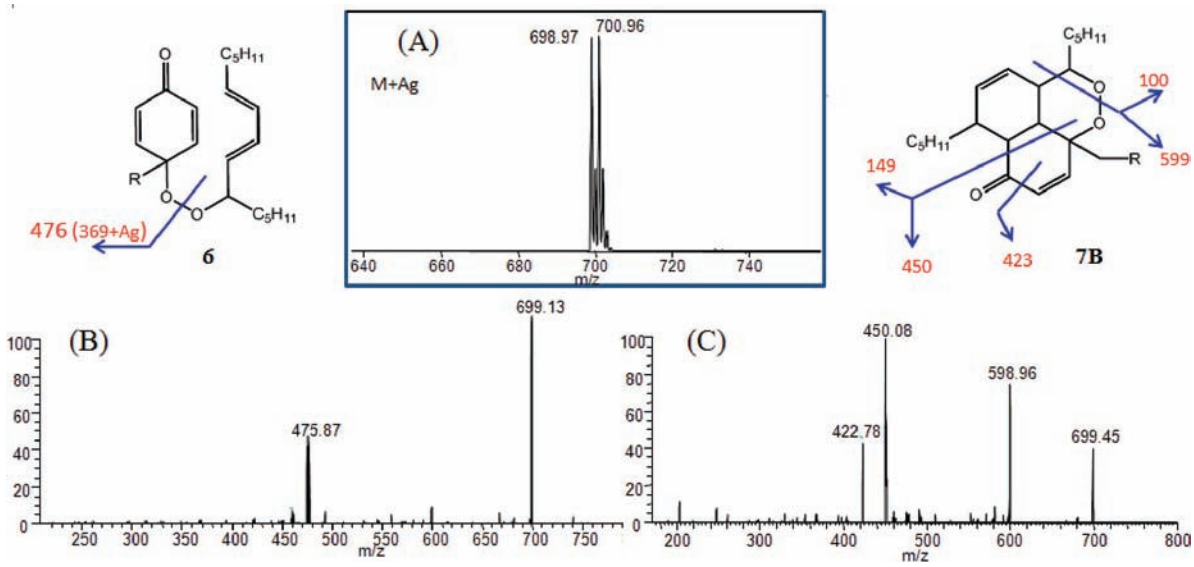

Figure 4. Representative MS spectra of primary and IMDA adducts in 1 μM $AgNO_3$ in MeOH sprayed directly into the MS source (collision pressure, 1.40 mTorr; collision dissociation energy, 25 eV): (A) precursor masses of the primary and IMDA adducts [M+Ag] at *m*/*z* 699 and 701; (B) CID of the silver ion complex of primary adduct **6** at *m*/*z* 699; (C) CID of IMDA adduct **7b**.

4B). On the other hand, the silver ion complex of the cyclic adduct exhibited multiple fragmentations, as assigned in Figure 4C.

Kinetics of the Intramolecular Diels−Alder Reaction of Adduct 6. Rate constants for the IMDA reaction under several sets of conditions were determined. The transformation was monitored at 231 nm, the λ_{max} of the conjugated diene (7′*E*,9′*E*)-pentadecadiene. The decrease in absorbance at 231 nm was due to loss of the conjugated diene as the reaction proceeded, as shown in Figure 5. The data fit a single-exponential decay, indicating a first-order process with a rate constant (k) of $(9 \pm 1) \times 10^{-5}$ s^{-1} in ethanol at 37 °C. The rate constant was lower in aprotic solvents such as acetonitrile [$k = (6.8 \pm 0.8) \times 10^{-5}$ s^{-1}] and hexanes [$k = (1.3 \pm 0.3) \times 10^{-5}$ s^{-1}] at 37 °C, also having an apparent correlation with polarity. Eyring analysis gave $\Delta H^{\ddagger} = 68$ kJ mol^{-1} and $\Delta S^{\ddagger} = -98$ J K^{-1} mol^{-1} in ethanol in the 25−50 °C range.

Reduction of Adduct 6. While a rich chemistry is expected for **6**, we limited the scope of our current studies to an exploration of reduction reactions leading to stable end products. Thus, reaction of **6** with cuprous ion or thiourea gave the *p*-hydroxycyclohexadienone **11** in modest yield:

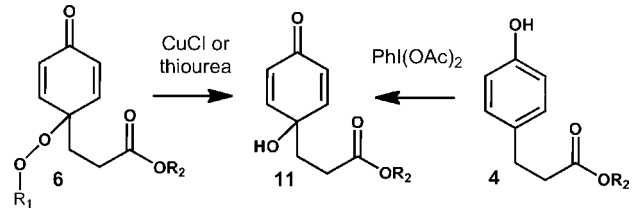

We found no evidence for the formation of *o*-hydroquinone **12** in the crude product mixture formed from co-oxidation of **4** and **5**, which also suggests that coupling of the peroxyl radical is exclusively para. Cuprous ion was found to be the most effective way to reduce **6**, while ferrous salts, thiourea, and glutathione generated some compound **11**, albeit in low yield. The *p*-OH product **11** was independently synthesized by the reaction of phenol precursor **4** with $PhI(OAc)_2$.[44,45] The isomeric hydroquinone **12** was also independently synthesized, so authentic standards of both products were available for comparison.

(44) Wipf, P.; Kim, Y. *Tetrahedron Lett.* **1992**, *33*, 5477.
(45) Pelter, A.; Satchwell, P.; Ward, R. S.; Blake, K. *J. Chem. Soc., Perkin Trans. 1* **1995**, 2201.

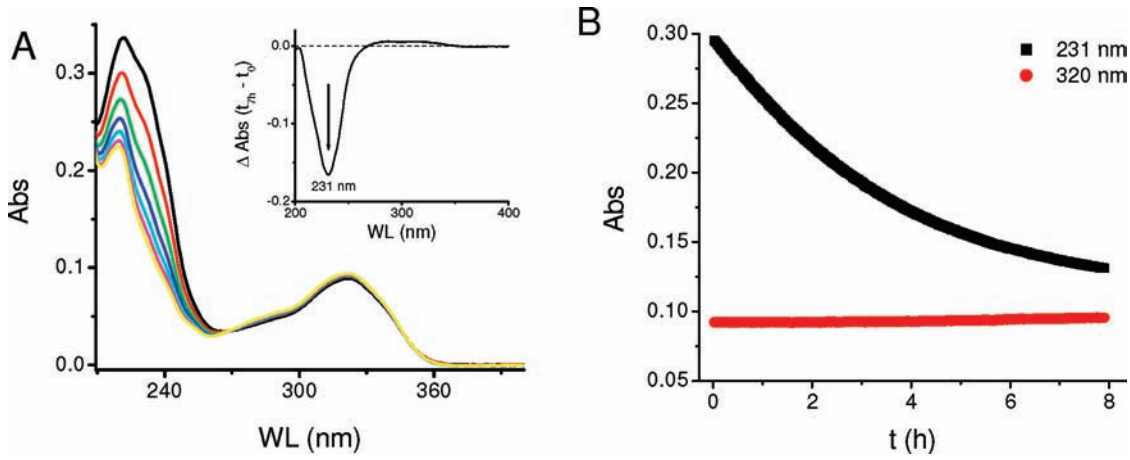

Figure 5. Kinetics of the intramolecular Diels−Alder reaction of adduct **6** in ethanol at 37 °C. (A) Spectra collected every 1 h. The inset shows the difference between the spectra recorded at $t = 7$ h and the initial time. (B) Fit of the decay at 231 nm to a single-exponential function, indicating a first-order reaction with rate constant $k = (9 \pm 1) \times 10^{-5}$ s^{-1} ($n = 3$). The absorbance at 320 nm (coumarin moiety) remained constant and was used as a normalizing element.

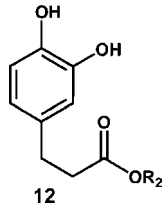

12

Co-oxidation of Tyrosine Derivatives with Methyl Linoleate. The formation and isolation of phenoxy−peroxyl radical cross-termination products in the simple model system served as a template for the reaction of more complex systems, including *N*-acetyltyrosine ethyl ester **13** and the tyrosine−alanine dipeptide **14**. Reaction of both substrates with methyl linoleate gave rise to adducts that had the mass spectra appropriate for the tyrosyl−linoleate peroxyl radical cross-termination product, and the dipeptide system was subjected to a more detailed analysis. The primary product of co-oxidation of methyl linoleate and dipeptide **14** had a UV λ_{max} at 235 nm, indicating the presence of a conjugated diene; the molecular ion was observed at *m*/*z* 633.4 (Figure S13 in the Supporting Information), and NMR analysis indicated the presence of a major product or mixture of major products having a ^{13}C chemical shift for a carbonyl carbon at ∼185 ppm and 2D spectra consistent with the formation of a product or products having a structure analogous to **6** (Figure S15 in the Supporting Information). It should be noted that four linoleate hydroperoxide stereoisomers are formed in the peroxidation reaction, and four coupling products with structures analogous to **6** are thus likely to be formed. This accounts for the complexity of the product mixture as analyzed by NMR spectroscopy and HPLC. Products were also found in the reaction mixture of **14** and methyl linoleate that had a ^{13}C chemical shift for a carbonyl carbon at 196−198 ppm and 2D spectra consistent with formation of a product or products having structures analogous to **7a**−**c**.

Reaction of the linoleate−peroxyl adduct mixture of **14** with CuCl gave rise to the 4-hydroxycyclohexa-2,5-dione **15** (Figure S18 in the Supporting Information), a product that was synthesized independently by reaction of **14** with PhI(OAc)$_2$.[44,45] The chromatogram shown in Figure 6 illustrates the fact that the para-coupling product is the only adduct formed. Chromatograms D and E in Figure 6 show an analysis of the reaction product formed from dipeptide **14** and methyl linoleate scanned

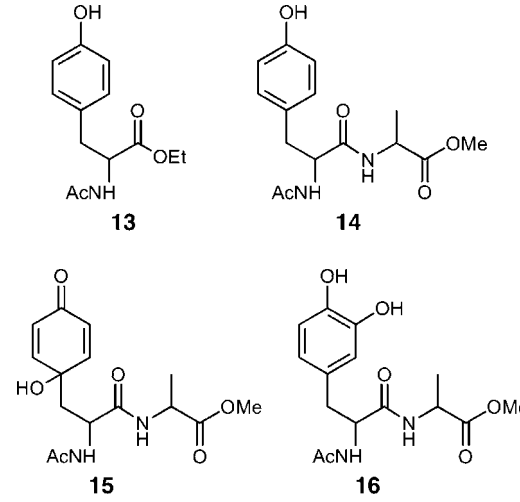

for the [M + 18] adduct (D) before and (E) after reaction with CuCl. Chromatogram B shows a synthetic standard of *o*-hydroquinone **16**, and the synthetic *p*-hydroxytyrosyl dipeptide **15** is shown in chromatogram C. Clearly, there is no evidence for the formation of the hydroquinone that would be produced by ortho coupling. In summary, all of the data gathered from

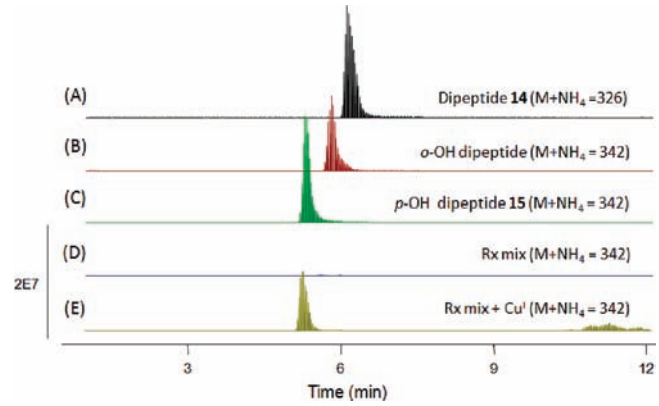

Figure 6. Extracted ion chromatograms of the CuCl reduction mixture of **14**−linoleate adducts: (A) **14**; (B) synthetic **16**; (C) synthetic **15**; (D) crude co-oxidation mixture before reduction; (E) crude co-oxidation mixture after CuCl reduction.

Scheme 3. Radical Termination Products of *p*-Cresol and *tert*-Butyl Hydroperoxide

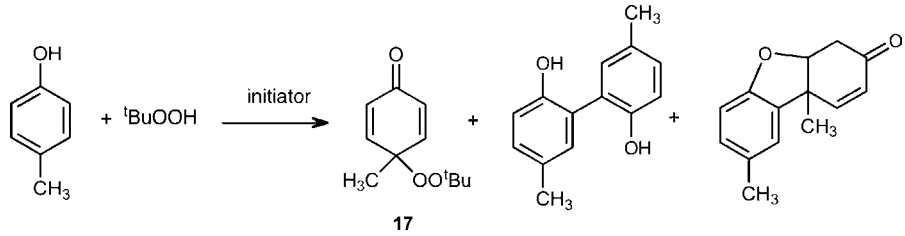

the reaction of **14** and methyl linoleate are consistent with the formation of para cross-termination primary products in this co-oxidation.

Discussion

Phenolic antioxidants trap peroxyl radicals in a two-step sequence: the first step is an H-atom transfer from phenol to the peroxyl radical (eq 1),

$$\mathrm{ArOH} + \mathrm{ROO}^{\bullet} \xrightarrow{k_{\mathrm{inh}}} \mathrm{ArO}^{\bullet} + \mathrm{ROOH} \qquad (1)$$

and the second is the reaction of the intermediate phenoxy radical with another peroxyl radical to give nonradical products (eq 2).

$$\mathrm{ArO}^{\bullet} + \mathrm{ROO}^{\bullet} \rightarrow \text{nonradical products} \qquad (2)$$

Nature's phenolic antioxidant, α-tocopherol, reacts with peroxyl radicals with a rate constant for inhibition (k_{inh}) of over 2×10^6 M^{-1} s^{-1}, and the second step, a radical−radical coupling, occurs with a rate close or equal to the diffusion-controlled value. The inhibition rate constant k_{inh} depends dramatically on the nature of the substituents on the phenol. Tyrosine, a para-substituted alkylphenol, has a bond dissociation enthalpy of 85.2 kcal/mol,[46] which is nearly 9 kcal/mol higher than that of tocopherol, and as expected, the inhibition rate constant recently reported for tyrosine is substantially less than that of tocopherol.[9,47] Nevertheless, as a *p*-alkylphenol, tyrosine is expected to be a modestly active antioxidant and trap peroxyl radicals to give nonradical termination products.

The phenolic radical termination step leading to nonradical products has been studied in some detail for α-tocopherol as well as for commercial products such as butylated hydroxytoluene (BHT), butylated hydroxyanisole (BHA), and simple phenols.[36] The termination products observed are usually the result of peroxyl coupling at the para and ortho positions of the aryloxy ring. Simple phenols such as *p*-cresol give cross-coupling products with *tert*-butylperoxyl radicals bonded exclusively at the para position (see Scheme 3). Products from aryloxy radical dimerization are also formed, but the cross-coupling product **17** is the major product formed under most reaction conditions.[36] In view of this precedent, it is notable that cross-termination products of tyrosine, itself a *p*-alkylphenol, and lipid peroxyl radicals have not been previously detected in extracts from cells, tissues, and biological fluids. One suspects that the primary peroxide coupling products may not survive biological reducing agents present in fluids and tissues, and for this reason, we chose to examine tyrosyl−peroxyl radical coupling at the fundamental chemical level with the idea that the knowledge gained from this study could be used in studies of relevant biological systems.

The free-radical-initiated reaction of the hydrophobic tyrosine BTBE and the phospholipid hydroperoxide PLPC-(13*S*)-OOH did indeed give a product fraction having the correct *m*/*z* in the precursor-ion mass spectrum as well as an MS^2 fragmentation pattern consistent with an adduct of tyrosine and peroxide. The isolation of homogeneous products from BTBE proved difficult, but co-oxidation of simple phenol **4** and symmetrical diene **5** did give sufficient quantities of adducts for a comprehensive NMR study. The major product identified at early stages of the reaction was the peroxide para-coupling product **6**, with no evidence for the formation of the phenol dimer or ortho-coupling products. The peroxide **6** slowly undergoes an intramolecular Diels−Alder reaction to give at least three tricyclic products, with one of the endo stereoisomers, **7b**, as the major IMDA product formed. We note that while the half-life for IMDA cyclization at 37 °C is on the order of 2 h, the rate is solvent-dependent and likely subject to acid catalysis. Of particular note is the fact that the IMDA reaction leads to new C−C bonds between the lipid and phenol (or tyrosine). Thus, while the peroxide bond of a lipid−protein adduct such as **6** should be readily reduced and the lipid−protein bond severed, any IMDA lipid−protein coupling products formed are more likely to be of a permanent nature.

Peroxyl radical coupling with phenoxy radicals followed by IMDA cycloaddition has been reported in the reactions of curcumin[39,40] as well as caffeic[41] and ferulic acid[42,43] esters. Caffeic acid, curcumin, and ferulic acid have phenol ring substitution as in **18**, and the products that have been isolated appear to be the result of ortho coupling to the phenolic OH. The preference for ortho coupling in **18** is likely due to the fact that para coupling in **18** would disrupt the olefin conjugation; this is not the case for tyrosine, which has para alkyl substitution.

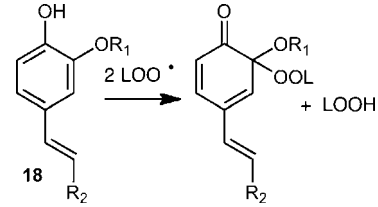

The system studied in detail, **4** + **5** → **6**, does serve as a model for the reactions of systems more relevant to proteins and fatty acids. Thus, the data accumulated from the reactions of **13** or **14** with methyl linoleate gave evidence of a linoleate−tyrosine para adduct. While the product mixture was complex and adducts could not be isolated in pure form, characteristic MS, MS^2, and NMR data were acquired and indicated that the chemistry observed in the model system translates to the more complex peptide−lipid reactions. Evidence for the formation of para adducts and reduction of the primary products to the 4-hydroxycyclohexa-2,5-dienone was obtained.

(46) Nara, S. J.; Valgimigli, L.; Pedulli, G. F.; Pratt, D. A. *J. Am. Chem. Soc.* **2010**, *132*, 863.
(47) Jha, M.; Pratt, D. A. *Chem. Commun.* **2008**, *10*, 1252.

Scheme 4. Tyrosine Lipid-Mediated Protein Cross-Link

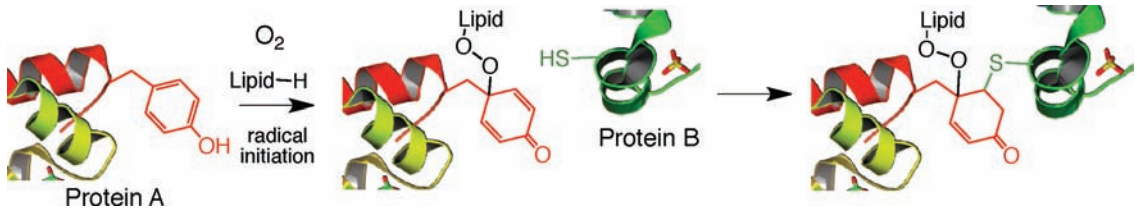

We note that both the lipid peroxide−tyrosine adducts, any derived 4-hydroxycyclohexadienones, and the IMDA cycloadducts are electrophiles and should be subject to attack by nucleophiles from proteins or nucleic acids. Cross-conjugated cyclohexadienones are prone to undergo Michael addition, and cysteines, lysines, and histidines are potential protein-derived nucleophiles. A Michael addition of a cysteine on one protein and a tyrosine-derived electrophile on another would lead to a protein−lipid−protein adduct, which could account for the formation of high-molecular-weight protein species in systems under conditions of oxidative stress, as shown in Scheme 4.

High-molecular-weight protein−protein adducts are frequently found under conditions of oxidative stress, and tyrosyl−tyrosyl radical coupling has been cited as one mechanism for formation of these adducts.[8,18,19,25,32,33,48−51] We suggest that lipid peroxide−tyrosine adducts such as those reported here are also likely sources of such high-molecular-weight protein species under conditions of oxidative stress. Oxidizable lipids are likely to be present in great excess relative to tyrosine residues in biological membranes, which are known targets of reactive oxygen species. The formation of lipid-derived peroxyl radicals is in fact one of the cornerstone reactions of oxidative stress, and these lipid peroxyls are relatively mobile in a membrane in comparison with a tyrosine protein residue.[52]

Tyrosine radical−peroxyl radical chemistry is likely to be dependent on the local protein−lipid environment, including the presence or absence of antioxidant inhibitors. Tyrosine gives up its phenolic hydrogen some 3 orders of magnitude slower than does α-tocopherol, so it seems likely that tyrosine radical chemistry will be suppressed if tocopherol is present in a lipid membrane or compartment. However, circumstances exist where tocopherol intervention in tyrosine−lipid free radical chemistry seems unlikely, one such instance being in HDL biology. HDL plays an important role in reverse-cholesterol transport, and oxidative modification of HDL particles has been suggested to play a role in the development of cardiovascular disease.[19,32,34,48,49,51,53,54] An average HDL particle has a molecular weight of 270 kD, of which 50% is protein and 28% phospholipid. HDL contains on average ∼0.67 molecules of α-tocopherol per particle.[53] This means that one in three HDL particles should have no α-tocopherol, while each should contain ∼98 molecules of phospholipid and 30−40 tyrosine residues (see the Supporting Information for calculations that lead to this estimate).[34,53] In those particles that contain no α-tocopherol, unsaturated lipids and tyrosine protein residues are among the most likely targets of peroxyl radical attack.

Once membrane or lipoprotein tyrosyl radicals are formed, their fate is determined by whether the radical first encounters another tyrosyl radical and undergoes self-termination to give a tyrosine−tyrosine dimer or instead finds a lipid peroxyl radical to give a cross-termination product. Our studies in homogeneous solution found significant amounts of cross-termination products under conditions where the oxidizable lipid is present in excess relative to the phenol. It seems reasonable to suggest that many biological membranes and lipid particles provide local environments in which tyrosyl−tyrosyl radical coupling is limited by the specific sites and rate of diffusion of these protein radicals. Lipid peroxyl radicals, on the other hand, would likely be substantially more mobile than protein tyrosine radicals, perhaps by 2 or 3 orders of magnitude, and this should promote the cross-termination reaction.[52,55−58]

Finally, we note that the focus of a host of studies on protein tyrosine modification has mainly centered on ortho substitution (i.e., chlorination, hydroxylation, and nitration). The stable lipid peroxide−tyrosine adducts identified here resulted exclusively from para addition to the tyrosine moiety, which suggests that para-substituted products may also be formed in other radical transformations. Such para-addition compounds would be active electrophiles and subject to reaction with protein and nucleic acid nucleophiles. Numerous reports have suggested that oxidation and adduction of tyrosines might play an important role in numerous diseases, including atherosclerosis[25,26,33,59,60] and neurodegenerative disorders such as Parkinson's and Alzheimer's diseases.[27−31,61−75] We suggest that lipid and lipid peroxyl radicals[76] may play an important role in this chemistry.

Experimental Section

General Methods and Materials. BTBE was prepared by Dr. Joy Joseph of the Medical College of Wisconsin. The initiator

(48) Shao, B.; Heinecke, J. W. *J. Lipid Res.* **2009**, *50*, 599.
(49) Shao, B.; Tang, C.; Heinecke, J. W.; Oram, J. F. *J. Lipid Res.* [Online early access]. DOI: 10.1194/jlr.M004085. Published Online: Jan 11, 2010.
(50) Chen, X.; Zhang, W.; Laird, J.; Hazen, S. L.; Salomon, R. G. *J. Lipid Res.* **2008**, *49*, 832.
(51) Peng, D.; Brubaker, G.; Wu, Z.; Zheng, L.; Willard, B.; Kinter, M.; Hazen, S. L.; Smith, J. D. *Arterioscler., Thromb., Vasc. Biol.* **2008**, *28*, 2063.
(52) Melo, E.; Martins, J. *Biophys. Chem.* **2006**, *123*, 77.
(53) Perugini, C.; Bagnati, M.; Cau, C.; Bordone, R.; Paffoni, P.; Re, R.; Zoppis, E.; Albano, E.; Bellomo, G. *Pharmacol. Res.* **2000**, *41*, 67.
(54) Szapacs, M. E.; Kim, H.; Porter, N. A.; Liebler, D. C. *Int. J. Proteome Res.* **2008**, *7*, 4237.
(55) Sackmann, E.; Trauble, H.; Galla, H. J.; Overath, P. *Biochemistry* **1973**, *12*, 5360.
(56) Sonnen, A. F.-P.; Bakirci, H.; Netscher, T.; Nau, W. M. *J. Am. Chem. Soc.* **2005**, *127*, 15575.
(57) Vanderkooi, J. M.; Callis, J. B. *Biochemistry* **1974**, *13*, 4000.
(58) Pali, T.; Horvath, L. I. *Acta Physiol. Hung.* **1989**, *74*, 311.
(59) Polymeropoulos, M. H.; et al. *Science* **1997**, *276*, 2045.
(60) Souza, J. M.; Giasson, B. I.; Chen, Q.; Lee, V. M. Y.; Ischiropoulos, H. *J. Biol. Chem.* **2000**, *275*, 18344.
(61) Benner, E. J.; Banerjee, R.; Reynolds, A. D.; Sherman, S.; Pisarev, V. M.; Tsiperson, V.; Nemachek, C.; Ciborowski, P.; Przedborski, S.; Mosley, R. L.; Gendelman, H. E. *PLoS One* **2008**, *3*, e1376.
(62) AbdAlla, S.; Lother, H.; el Missiry, A.; Sergeev, P.; Langer, A.; el Faramawy, Y.; Quitterer, U. *J. Biol. Chem.* **2009**, *284*, 6566.

MeOAMVN was purchased from Wako Chemicals USA, Inc. (Richmond, VA) and dried under high vacuum for 2 h and kept at −80 °C until use. Methyl linoleate and linoleic acids were purchased from NuChek Prep (Elysian, MN). Symmetric (6*E*,9*E*)-pentadecadiene was synthesized following the method reported previously.[38] Benzene (HPLC grade) was passed through a column of neutral alumina and stored over molecular sieves. Hexanes, ethyl acetate, methylene chloride, tetrahydrofuran (THF), and methanol (all 99.9%) were purchased from Thermo Fisher Scientific Inc. Lipids were obtained from Avanti Polar Lipids, and 3-(4-hydroxyphenyl)-propionic acid and 4-bromomethyl-7-methoxycoumarin were purchased from TCI America. 4-Dihydroxyhydrocinnamic and L-alanine methyl ester hydrochloride were purchased from Sigma-Aldrich. *N*-Acetyl-L-tyrosine was purchased from Fluka. $PhI(OAc)_2$ (iodobenzene diacetate) was purchased from Acros Organics. Triethylamine and *N*,*N*-dimethylformamide (DriSolv) were purchased from EMD and used without further purification. All glassware was oven-dried prior to use.

HPLC Analysis Conditions. NP HPLC analyses were performed using a Beckman Ultrasphere 5 μm silica column (4.6 mm × 25 cm) using different methods: condition A: isocratic method using 20% ethyl acetate in hexanes at a flow rate of 1.5 mL/min; condition B: 10% isopropyl alcohol in hexanes increasing to 15% isopropyl alcohol over 15 min and remaining there for 5 min; condition C: 8% isopropyl alcohol in hexanes at 4 mL/min using a semipreparative NP column (Beckman Ultrasphere Silica 5 μm, 10 mm × 25 cm). RP HPLC analyses were performed using a Luna C-18 column (4.6 mm × 25 cm) from Phenomenex (Torrance, CA). The mobile phases used in RP HPLC were: condition 1: (A) 10 mM ammonium formate and (B) acetonitrile, with an initial gradient of 80% B that was increased to 95% B immediately followed by 99% B for 10 min; condition 2: (A) 10 mM NH_4OAc in H_2O and (B) 10 mM NH_4OAc in 95% CH_3OH/H_2O, with a gradient that started with 70% B, was increased to 100% B over 10 min, and was maintained at 100% B for 15 min; condition 3: (A) 10 mM ammonium formate and (B) acetonitrile, with a gradient that started at 25% B for 5 min, was increased to 50% B for 5 min and then to 75% B for 5 min, which was followed immediately by 99% B for 5 min; condition 4: starting with 70% acetonitrile/10 mM ammonium formate, increasing to 83% acetonitrile over 20 min, and then returning to 70% acetonitrile.

NMR Studies. All of the reported NMR spectra were acquired using a 14.1 T Bruker magnet equipped with a Bruker DRX spectrometer operating at a proton Larmor frequency of 600.13 MHz. ^1H spectra were acquired in 2.5 mm NMR tubes using a Bruker 5 mm cryogenically cooled NMR probe. Chemical shifts were referenced internally to chloroform (7.26 ppm), which also served as the ^2H lock solvent. ^1H, 2D COSY, NOESY, HSQC, and HMBC spectra were obtained for all of the adducts for structural assignments. ^{13}C spectra were obtained only for the major adducts. Some NMR spectra were interpreted using MestReNova NMR 6.1.1.

Silver-Coordinated (LC−Ag^+)-CID-MS of Acyclic and Cyclic Adducts. The adducts were purified by HPLC prior to MS analysis and then dissolved in 0.3 mM $AgNO_3$ solution in MeOH to obtain MS2 information.[77] MS was performed using a Thermo Finnigan TSQ Quantum Ultra instrument equipped with a Finnigan Surveyor Autosampler Plus (San Jose, CA). Nitrogen gas served both as the sheath and auxiliary gas, and argon served as the collision gas. The electrospray needle was maintained at 4.6 kV, and the heated capillary temperature was 200 °C. CID of the tyrosine adducts was set at either 25 or 35 eV under 1.4 mTorr of argon. In the displayed spectra, the scans were averaged across the individual chromatography peaks. Data acquisition and analysis was performed using Xcalibur software, version 2.0 SR2 (San Jose, CA).

HPLC−ESI Mass Spectrometry. HPLC−MS/MS analysis was performed on a Waters Aquity UPLC system (Waters, Milford, MA) connected to a Finnigan LTQ mass spectrometer (Thermo Fisher Scientific, Waltham, MA) operating in the ESI positive-ion mode. The same HPLC mobile phases and gradients described above were used for the LC−MS analysis, but a different column, Luna C8 with 3 μm at a flow rate of 350 μL/min, was employed. MS analysis was performed in both data-dependent and selected-ion-monitoring (SIM) mode for the desired *m*/*z*.

Synthesis of PLPC-(13*S*)-OOH (2). PLPC (5 mg) and 4 mg of soybean lipoxygenase (Sigma, St. Louis, MO) were dissolved in 5 mL of 100 mM borate/10 mM deoxycholic acid buffer (pH 9). The reaction mixture was stirred vigorously at room temperature for 1 h, after which 2:1 $CHCl_3/CH_3OH$ was used twice (3 mL each) to extract PLPC and PLPC-OOH. The organic layer was collected and the solvent evaporated using a rotary evaporator. The phospholipid extracted in this way was resuspended in CH_3OH and purified with HPLC using 95% CH_3OH in H_2O as the solvent. The collected peak was dried and resuspended in isopropyl alcohol for use as a stock solution (2.16 mg/4 mL).

Oxidation of BTBE (1) and PLPC-(13*S*)-OOH (2) in a Liposome. BTBE (33.7 mg) was dissolved in 1 mL of CH_3OH to prepare a 100 mM stock solution. PLPC-(13*S*)-OOH stock solution (1 mL, 540 μg of **2**) and BTBE stock solution (2 μL) were combined in an Eppendorf tube, and 2 μL of MeOAMVN stock solution (50 mM in benzene) was added. The solution was vortexed for 2 min and then dried under a nitrogen stream. NH_4OAc (100 μL of a 100 mM solution, pH 7) was added to the dried mixture to make a solution with final **2**, **1**, and MeOAMVN concentrations of 6.8, 2, and 1 mM respectively. The reaction mixture was sonicated for 5 min and then allowed to stand in a 37 °C sand bath with stirring. An aliquot (30 μL) was taken from the reaction mixture after 4 h and diluted with 100 μL of CH_3OH for MS analysis.

Synthesis of Tyrosine Analogue 4. To a 100 mL round-bottom flask was added 3-(4-hydroxyphenyl)propionic acid (0.62 g, 3.72 mmol), and the flask was purged with argon. DMF (40 mL) and then 4-bromomethyl-7-methoxycoumarin (1.0 g, 3.7 mmol) followed by triethylamine (0.52 mL, 3.7 mmol) were added. The flask was wrapped with aluminum foil and stirred at room temperature under an argon balloon for 24 h. The solvent was then removed in vacuo, yielding the crude product as a pale-brown oil. Silica flash column chromatography (60:39:1 hexanes/EtOAc/TEA) afforded the product, **4**, as a white solid (1.15 g, 87%) upon solvent removal. ^1H NMR (400 MHz, DMSO): δ 9.17 (s, 1H), 7.58 (d, J = 8.9 Hz, 1H), 7.05−6.98 (m, 3H), 6.94 (dd, J = 8.9, 2.5 Hz, 1H), 6.72−6.59

(63) Ali, F. E.; Leung, A.; Cherny, R. A.; Mavros, C.; Barnham, K. J.; Separovic, F.; Barrow, C. J. *Free Radical Res.* **2006**, *40*, 1.
(64) Danielson, S. R.; Held, J. M.; Schilling, B.; Oo, M.; Gibson, B. W.; Andersen, J. K. *Anal. Chem.* **2009**, *81*, 7823.
(65) Good, P. F.; Hsu, A.; Werner, P.; Perl, D. P.; Olanow, C. W. *J. Neuropathol. Exp. Neurol.* **1998**, *57*, 338.
(66) Pennathur, S.; Jackson-Lewis, V.; Przedborski, S.; Heinecke, J. W. *J. Biol. Chem.* **1999**, *274*, 34621.
(67) Schulz, J. B.; Matthews, R. T.; Muqit, M. M.; Browne, S. E.; Beal, M. F. *J. Neurochem.* **1995**, *64*, 936.
(68) Anantharaman, M.; Tangpong, J.; Keller, J. N.; Murphy, M. P.; Markesbery, W. R.; Kiningham, K. K.; St. Clair, D. K. *Am. J. Pathol.* **2006**, *168*, 1608.
(69) Butterfield, D. A.; Reed, T. T.; Perluigi, M.; De Marco, C.; Coccia, R.; Keller, J. N.; Markesbery, W. R.; Sultana, R. *Brain Res.* **2007**, *1148*, 243.
(70) Good, P. F.; Werner, P.; Hsu, A.; Olanow, C. W.; Perl, D. P. *Am. J. Pathol.* **1996**, *149*, 21.
(71) Hensley, K.; Maidt, M. L.; Yu, Z.; Sang, H.; Markesbery, W. R.; Floyd, R. A. *J. Neurosci.* **1998**, *18*, 8126.
(72) Reynolds, M. R.; Berry, R. W.; Binder, L. I. *Biochemistry* **2005**, *44*, 1690.
(73) Reynolds, M. R.; Lukas, T. J.; Berry, R. W.; Binder, L. I. *Biochemistry* **2006**, *45*, 4314.
(74) Smith, M. A.; Richey Harris, P. L.; Sayre, L. M.; Beckman, J. S.; Perry, G. *J. Neurosci.* **1997**, *17*, 2653.
(75) Tohgi, H.; Abe, T.; Yamazaki, K.; Murata, T.; Ishizaki, E.; Isobe, C. *Neurosci. Lett.* **1999**, *269*, 52.
(76) Spiteller, G. *Free Radical Biol. Med.* **2006**, *41*, 362.
(77) Havrilla, C. M.; Hachey, D. L.; Porter, N. A. *J. Am. Chem. Soc.* **2000**, *122*, 8042.

(m, 2H), 6.23 (s, 1H), 5.31 (d, $J = 1.1$ Hz, 2H), 3.85 (s, 3H), 2.75 (tt, $J = 6.8$, 3.4 Hz, 4H). ^{13}C NMR (101 MHz, DMSO): δ 172.29, 162.90, 160.29, 156.03, 155.35, 150.72, 130.69, 129.49, 126.20, 115.48, 112.69, 110.67, 109.58, 101.38, 61.54, 56.35, 35.60, 29.78. HRMS (M + Na) *m*/*z*: calcd, 377.0996; found, 377.0996.

Oxidation of Tyrosine Analogue 4 with (6*E*,9*E*)-Pentadecadiene (5). To a solution of **5** (0.5 g, 2.4 mmol) in benzene (3 mL) at 37 °C were added a solution of **4** (21 mg, 0.06 mmol in 2 mL of MeCN) and the radical initiator MeOAMVN (30 mg, 0.1 mmol). The reaction mixture was kept at 37 °C under an oxygen atmosphere for 9 h. Reaction progress was monitored by HPLC after 5 h of oxidation. The reaction was stopped at 9 h to obtain pure acyclic adduct **6** for NMR experiments (Table S1 in the Supporting Information). HRMS (M + H) *m*/*z*: calcd, 593.3114; found 593.3107.

Kinetics of the Intramolecular Diels−Alder Reaction of Adduct 6. Adduct **6** was purified by NP HPLC using 20% ethyl acetate in hexanes. The peak corresponding to the acyclic adduct was collected, and its purity was assessed by RP HPLC and NMR spectroscopy. In order to assess the rate of cyclization from adduct **6** to **7** via IMDA reaction, a small volume of the work solution was introduced into a much larger volume of solvent that had been pre-equilibrated at the desired temperature, yielding a final **6** concentration of 50 μM. The conversion was followed by UV spectroscopy in an Agilent 8453 photodiode-array spectrophotometer in quartz cuvettes with Teflon stoppers. The temperature was maintained at 37 °C by a circulating bath. The absorbance of the solution was measured at 231 nm, the λ_{max} of the conjugated diene, every 2 min for 8 h. The decrease in absorbance at 231 nm was fitted to a single-exponential decay.

Reduction of Adduct 6. To 100 μL aliquots of a 100 μM solution of **6** in 10% isopropyl alcohol in ethyl acetate were added a variety of reducing reagents. Thus, the following reagents were examined in exploratory experiments: (A) 5 mg of CuCl crystals; (B) 5 mg of $Fe(NH_4)_2(SO_4)_2$; (C) 10 mM thiourea in methanol; (D) 5 mg of CuCl crystals and 8.4 M acetic acid; (E) 5 mg of $Fe(NH_4)_2(SO_4)_2$ and 8.4 M acetic acid; (F) 5 mg of Zn dust and 8.4 M acetic acid;[78] (G) 20 μM $CuSO_4$ and 100 μM or 1 mM ascorbic acid; (H) freshly scratched Mg turnings and iodine (in methanol); (I) dimethyl sulfide at 1, 10, and 100 mM; (J) 100 mM 2-mercaptoethanol; (K) glutathione at 1 and 100 mM; (L) sodium borohydride at 1 and 35 mM; and (M) 60 mM $SnCl_2$. Each reaction was left at room temperature for 18 h in the dark and then analyzed by RP HPLC on a C18 column using solvent condition 3. The reaction progress was monitored at 320 nm. The reaction mixtures were compared with authentic standards of tyrosine analogue **4**, *p*-hydroxytyrosine analogue **11**, and *o*-hydroxytyrosine analogue **12**.

Synthesis of *o*-Hydroxytyrosine Analogue 12. To a 100 mL round-bottom flask under argon were added 3,4-dihydroxyhydrocinnamic acid (0.71 g, 3.90 mmol) and DMF (50 mL). To this solution was added 4-bromomethyl-7-methoxycoumarin (0.91 g, 3.38 mmol) followed by triethylamine (0.57 mL, 3.72 mmol). The reaction mixture turned light-yellow upon addition of the amine. The flask was wrapped with aluminum foil and stirred at room temperature under an argon balloon for 24 h. The solvent was removed in vacuo, yielding the crude product as a brown oil. Silica flash column chromatography (60:39:1 hexanes/EtOAc/TEA) afforded the product as a white solid (1.13 g, 90%) upon solvent removal. ^{1}H NMR (400 MHz, DMSO): δ 8.69 (s, 2H), 7.57 (d, $J = 8.9$ Hz, 1H), 7.02 (d, $J = 2.5$ Hz, 1H), 6.94 (dd, $J = 8.9$, 2.5 Hz, 1H), 6.60 (m, 2H), 6.45 (dd, $J = 8.0$, 2.1 Hz, 1H), 6.25 (s, 1H), 5.31 (d, $J = 1.0$ Hz, 2H), 3.85 (s, 3H), 2.71 (s, 4H). ^{13}C NMR (101 MHz, DMSO): δ 172.31, 162.90, 160.30, 155.36, 150.71, 145.45, 143.94, 131.45, 126.23, 119.14, 116.04, 115.84, 112.70, 110.69, 109.66, 101.40, 61.59, 56.36, 35.62, 30.00. HRMS (M + Na) *m*/*z*: calcd, 393.0945; found; 393.0938.

Oxidation of *N*-Acetyl-L-tyrosine Ethyl Ester (13) with Methyl Linoleate. Methyl linoleate (118 mg) and 5 mg of **13** were oxidized using 6 mg of MeOAMVN in 1 mL of 10% acetonitrile in benzene. The reaction mixture was fractionated using NP HPLC. The chromatograms of the adducts (Figure S10 in the Supporting Information) were similar to those of the adducts formed in the reaction of **4** and **5** but much more complex because of the formation of regioisomers. Fraction A was collected, dried under vacuum, resuspended in MeOH containing 0.1% acetic acid, and analyzed by MS. The corresponding adducts were identified [yielding (M + H) and (M + Na) peaks at *m*/*z* 575.93 and 598.27, respectively] and further characterized by MS^2 (Figure S11 in the Supporting Information).

Synthesis of the Dipeptide *N*-Acetyl-L-tyrosine-L-alanine Methyl Ester (14). To a flame-dried 10 mL round-bottom flask were added *N*-acetyl-L-tyrosine (0.50 g, 2.24 mmol), L-alanine methyl ester hydrochloride (0.31 g, 2.24 mmol), and 2-chloro-4,6-dimethoxy-1,3,5-triazine (CDMT) (0.433 g, 2.46 mmol).[79] The flask was dried in vacuo for 20 min and then purged with argon. Acetonitrile (2.5 mL) and then 4-methylmorpholine (NMM) (0.616 mL, 5.60 mmol) were added over 10 min, and the reaction was stirred at 15 °C under an argon balloon for 2 h. The reaction was quenched with H_2O (12 mL) and extracted with ethyl acetate (25 mL). The organic layer was washed with 1 N HCl (2×, 6 mL), H_2O (12 mL), and brine (12 mL), dried over $MgSO_4$, filtered, and concentrated in vacuo. Silica flash column chromatography (10:90 $MeOH/CH_2Cl_2$) afforded the product, **14**, as a white solid (0.50 g, 72.4%) upon solvent removal. ^{1}H NMR (400 MHz, DMSO): δ 9.13 (s, 1H), 8.41 (d, $J = 7.0$ Hz, 1H), 7.98 (d, $J = 8.5$ Hz, 1H), 7.02 (d, $J = 8.5$ Hz, 2H), 6.63 (d, $J = 8.5$ Hz, 2H), 4.43 (td, $J = 9.8$, 4.2 Hz, 1H), 4.26 (p, $J = 7.2$ Hz, 1H), 3.60 (s, 3H), 2.85 (dd, $J = 13.9$, 4.2 Hz, 1H), 2.57 (dd, $J = 13.9$, 10.1 Hz, 1H), 1.73 (s, 3H), 1.27 (d, $J = 7.3$ Hz, 3H). ^{13}C NMR (101 MHz, DMSO): δ 173.31, 171.97, 169.42, 156.09, 130.42, 128.41, 115.18, 55.28, 54.28, 52.23, 47.91, 37.23, 22.83, 17.24. HRMS (M + Na) *m*/*z*: calcd, 331.1264; found, 331.1255.

Synthesis of the *p*-Hydroxy Dipeptide *N*-Acetyl-L-*p*-hydroxytyrosine-L-alanine Methyl Ester (15). To a 10 mL round-bottom flask were added $PhI(OAc)_2$ (0.31 g, 0.973 mmol) and 20:80 H_2O/THF (3.0 mL) followed by dipeptide **14** (0.15 g, 0.486 mmol, in 3.0 mL of 20:80 H_2O/THF) over 10 min. The reaction mixture turned light-yellow upon initial dipeptide addition and then became amber in color. The reaction mixture was stirred under atmosphere at room temperature. Reaction progress was monitored via TLC (10:90 $MeOH/CH_2Cl_2$) for loss of the starting dipeptide. After 2 h, the reaction was deemed complete, and the solvent was removed in vacuo, yielding an orange solid. Silica flash column chromatography (5:95 $MeOH/CH_2Cl_2$) afforded the product, **15**, as white solid (0.11 g, 70%) upon solvent removal. ^{1}H NMR (600 MHz, $CDCl_3$): δ 7.08 (dd, $J = 10.4$, 3.1 Hz, 1H), 6.97 (d, $J = 6.8$ Hz, 1H), 6.91 (dd, $J = 10.3$, 3.1 Hz, 1H), 6.51 (d, $J = 7.2$ Hz, 1H), 6.24−6.16 (m, 2H), 4.73 (dd, $J = 13.3$, 6.1 Hz, 1H), 4.54 (p, $J = 7.2$ Hz, 1H), 3.77 (s, 3H), 3.66 (s, 1H), 2.37 (dd, $J = 14.8$, 5.6 Hz, 1H), 2.05 (s, 3H), 1.95 (dd, $J = 14.8$, 6.3 Hz, 1H), 1.44 (d, $J = 7.2$ Hz, 3H). ^{13}C NMR (151 MHz, $CDCl_3$): δ 184.78, 172.91, 170.68, 170.40, 149.86, 149.41, 128.24, 127.76, 68.15, 52.64, 49.12, 48.36, 43.56, 23.20, 17.97. HRMS (M + Na) *m*/*z*: calcd, 347.1214; found, 347.1210.

Synthesis of the *o*-Hydroxy Dipeptide *N*-Acetyl-L-*o*-hydroxytyrosine-L-alanine Methyl Ester (16). To a 25 mL round-bottom flask were added 3,4-dihydroxy-L-phenylalanine (0.50 g, 2.54 mmol) and deionized H_2O (6.0 mL). The flask was purged with argon, and acetic anhydride (Ac_2O) (5.0 mL, 50.71 mmol) was added over 1 h with an addition funnel. The reaction mixture changed from milky-white to colorless upon Ac_2O addition and then became a slurry after 30 min. After 2 h at room temperature, the solvent was removed in vacuo. Silica flash column chroma-

(78) Dai, P.; Dussault, P.; Trulinger, T. *J. Org. Chem.* **2004**, *69*, 2851.

(79) Smith, K. C.; White, R. L. *J. Nat. Prod.* **1995**, *58*, 1274.

tography (40:60 MeOH/CH_2Cl_2) afforded *N*-acetyl-3,4-dihydroxy-L-phenylalanine[79] as a sticky white solid (0.30 g, 49%). ^{1}H NMR (300 MHz, D_2O): δ 6.72 (d, J = 8.0 Hz, 1H), 6.66 (s, 1H), 6.56 (d, J = 8.1 Hz, 1H), 4.31−4.21 (m, 1H), 2.94 (dd, J = 14.1, 4.7 Hz, 1H), 2.67 (dd, J = 14.0, 8.6 Hz, 1H), 1.82 (s, 3H).

To a 10 mL round-bottom flask were added *N*-acetyl-3,4-dihydroxy-L-phenylalanine (0.298 g, 1.25 mmol), L-alanine methyl ester hydrochloride (0.17 g, 1.25 mmol), and CDMT (0.24 g, 1.37 mmol). The flask was dried in vacuo for 20 min and then directly purged with argon. Acetonitrile (3.0 mL) was added, followed by NMM (0.34 mL, 3.11 mmol) over 10 min.[80] The reaction mixture turned cloudy after the addition of NMM. The reaction mixture was stirred at 15 °C under an argon balloon for 2 h, and then the reaction mixture was quenched with H_2O (12 mL) and extracted with ethyl acetate (30 mL). The organic layer was washed with 1 N HCl (2×, 6 mL), H_2O (12 mL), and brine (12 mL), dried over $MgSO_4$, filtered, and concentrated in vacuo. Silica flash column chromatography (10:90 MeOH/CH_2Cl_2) afforded the product, **16**, as white solid (0.28 g, 70%) upon solvent removal. ^{1}H NMR (600 MHz, D_2O): δ 6.67 (d, J = 8.1 Hz, 1H), 6.59 (d, J = 1.7 Hz, 1H), 6.52 (dd, J = 8.1, 1.7 Hz, 1H), 4.29 (t, J = 7.7 Hz, 1H), 4.19 (q, J = 7.2 Hz, 1H), 3.50 (s, 3H), 2.73 (qd, J = 13.8, 7.8 Hz, 2H), 1.79 (s, 3H), 1.15 (d, J = 7.2 Hz, 3H). ^{13}C NMR (151 MHz, D_2O): δ 174.36, 173.85, 172.80, 143.78, 142.78, 128.76, 121.46, 116.79, 116.07, 55.11, 52.80, 48.45, 36.35, 21.48, 16.12. HRMS (M + Na) *m*/*z*: calcd, 347.1214; found, 347.1211.

Oxidation of Dipeptide 14 with Methyl Linoleate. Methyl linoleate (400 mg) and 20 mg of dipeptide **14** were oxidized using 20 mg of MeOAMVN in 3.5 mL of 60% acetonitrile in benzene. The reaction mixture was fractionated using NP HPLC. The chromatograms of the adducts were similar to those of the adducts formed in the reaction of **4** and **5** but much more complex because of the formation of regio- and stereoisomers (Figure S12 in the Supporting Information). Fractions 6_1, 6_2, 7_3, and 7_4 were collected from RP HPLC and analyzed by mass spectrometry. The corresponding adducts yielding (M + H) and (M + Na) peaks at *m*/*z* 633.08 and 649.75, respectively, were observed and further characterized by MS^2 (Figure S13 in the Supporting Information). Fractions 6_1 and 7_4 were collected, and their 1D and 2 D NMR spectra were acquired. A number of peroxyl−phenol coupled adducts were formed, and the new downfield-shifted ^{13}C signal in the HMBC spectrum indicated the formation of para acyclic and cyclic adducts, as demonstrated in the model system.

(80) Garrett, C. E.; Jiang, X.; Prasad, K.; Repic, O. *Tetrahedron Lett.* **2002**, *43*, 4161.

Acknowledgment. We are grateful to Dr. Joy Joseph of the Medical College of Wisconsin for a gift of BTBE. N.A.P. acknowledges funding from the National Science Foundation and support from the Center in Molecular Toxicology at Vanderbilt University (T32 ES007028, Training Program in Environmental Toxicology). Support from the Howard Hughes Medical Institute to R.R., the National Institutes of Health to B.K. and R.R. (2 R01Hl063119-05), and Agencia Nacional de Investigación e Innovación (ANII)/Fondo Clemente Estable to S.B. (FCE_362) is also acknowledged. S.B. was partially supported by a fellowship of ANII. R.R. is a Howard Hughes International Research Scholar.

Supporting Information Available: Tables of ^{1}H and ^{13}C NMR chemical shifts, 1D and 2D NMR spectra, HPLC−MS data, experimental details, and complete ref 59. This material is available free of charge via the Internet at http://pubs.acs.org.

JA106503A